

Towards the short-wavelength limit lasing at 1450 nm over ${}^4I_{13/2} \rightarrow {}^4I_{15/2}$ transition in silica-based erbium-doped fiber

Nan-Kuang Chen^{1,*}, Chi-Ming Hung², Sien Chi^{2,3}, and Yinchieh Lai²

¹Department of Electro-Optical Engineering, National United University, Miaoli, Taiwan 360, R.O.C.

²Department of Photonics & Institute of Electro-Optical Engineering, National Chiao Tung University, Hsinchu, Taiwan 300, R.O.C.

³Department of Electrical Engineering, Yuan Ze University, Chungli, Taiwan 320, R.O.C.

*Corresponding author: nkchen@nuu.edu.tw

Abstract: The transition rate of the stimulated emission at the higher energy levels of the excited states in a silica-based erbium-doped fiber can be enhanced by introducing fundamental-mode cutoff filtering mechanism. The electrons excited by optical pumping can more occupy the higher energy levels of the excited states when the transition rate for the lower energy levels (longer wavelengths) of the excited states is substantially suppressed. The achieved lasing wavelength can thus be moving toward the shorter wavelengths of the gain bandwidth. The laser transition between ${}^4I_{13/2} \rightarrow {}^4I_{15/2}$ multiplets of the silica-based erbium-doped fiber is known to emit fluorescence with the shortest wavelength around 1450 nm. We, for the first time, experimentally demonstrate a widely tunable fiber laser at the wavelength very close to 1450 nm by using a standard silica-based C-band erbium-doped fiber. The tuning range covers 1451.9-1548.1 nm, with the best temperature tuning efficiency as high as 57.3 nm/°C, by discretely introducing tunable fundamental-mode cutoff tapered fiber filters along a 16-m-long erbium-doped fiber under a 980 nm pump power around 200 mW. The signal-ASE-ratio can be higher than 45 dB whereas the FWHM of the laser lasing lights can be reduced below 0.2 nm by using an additional Fabry-Perot filter.

©2007 Optical Society of America

OCIS codes: (140.3510) Lasers, fiber; (060.2410) Fibers, erbium; (060.2320) Fiber optics amplifiers and oscillators; (170.1870) Dermatology; (999.9999) Fundamental-mode cutoff

References and links

1. D. Y. Paithankar, J. M. Clifford, B. A. Saleh, E. V. Ross, C. A. Hardaway, and D. Barnette, "Subsurface skin renewal by treatment with a 1450-nm laser in combination with dynamic cooling," *J. of Biomedical Opt.* **8**, 545-551 (2003).
2. N. Fournier, S. dahan, G. Barneon, S. diridollou, J. M. Lagarde, Y. Gall, and S. Mordon, "Nonablative remodeling: clinical, histologic, ultrasound imaging, and profilometric evaluation of a 1540 nm Er: glass laser," *Dermatol. Surg.* **27**, 799-806 (2001).
3. C. C. Wang, Y. M. Sue, C. H. Yang, and C. K. Chen, "A comparison of Q-switched alexandrite laser and intense pulsed light for the treatment of freckles and lentigines in Asian persons: A randomized, physician-blinded, split-face comparative trial," *J. of American Academy of Dermatology*, **54**, 804-810 (2006).
4. J. Rao and R. E. Fitzpatrick, "Use of the Q-switched 755-nm Alexandrite laser to treat recalcitrant pigment after depigmentation therapy for vitiligo," *Dermatol. Surg.* **30**, 1043-1045 (2004).
5. S. Shen, A. Jha, L. Huang, and P. Joshi, "980-nm diode-pumped Tm³⁺/Yb³⁺-codoped tellurite fiber for S-band amplification," *Opt. Lett.* **30**, 1437-1439 (2005).
6. E. R. M. Taylor, L. N. Ng, J. Nilsson, R. Caponi, A. Pagano, M. Potenza, and B. Sordo, "Thulium-doped tellurite fiber amplifier," *IEEE Photon. Technol. Lett.* **16**, 777-779 (2004).
7. Y. Akasaka and S. Yam, "Gain bandwidth expansion to S-plus band using fiber OPA pumped by gain-clamping signal of a GS-TDFA," in *Proc. of OFC 2002, ThGG30* (2002).

8. J. Zhang, S. Dai, S. Li, S. Xu, G. Wang, and L. Hu, "Characterization of broadband amplified spontaneous emission of erbium-doped tellurite fiber with D-shape cladding," *Mater. Lett.* **58**, 3532-3535 (2004).
9. J. Zhang, S. Dai, S. Xu, G. Wang, and L. Hu, "Fabrication and amplified spontaneous emission spectrum of Er³⁺-doped tellurite glass fiber with D-shape cladding," *J. Alloys Compd.* **387**, 308-312 (2005).
10. M. C. Ho, K. Uesaka, M. Marhic, Y. Akasaka, and L. G. Kazovsky, "200-nm-Bandwidth fiber optic amplifier combining parametric and Raman gain," *J. Lightwave Technol.* **19**, 977981 (2001).
11. E. Desurvire and J. R. Simpson, "Evaluation of ⁴I_{15/2} and ⁴I_{13/2} Stark-level energies in erbium-doped aluminosilicate glass fibers," *Opt. Lett.* **15**, 547-549 (1990).
12. N. K. Chen, K. C. Hsu, S. Chi, and Y. Lai, "Tunable Er³⁺-doped fiber amplifiers covering S and C + L bands over 1490-1610 nm based on discrete fundamental-mode cutoff filters," *Opt. Lett.* **31**, 2842-2844 (2006).
13. M. A. Arbore, Y. Zhou, H. Thiele, J. Bromage, and L. Nelson, "S-band erbium-doped fiber amplifiers for WDM transmission between 1488 and 1508 nm," in *Proc. of OFC 2003, WK2* (2003).
14. M. Foroni, F. Poli, A. Cucinotta, and S. Selleri, "S-band depressed-cladding erbium-doped fiber amplifier with double-pass configuration," *Opt. Lett.* **31**, 3228-3230 (2006).
15. E. Desurvire, *Erbium-doped fiber amplifiers: Principles and applications* (Wiley-Interscience, New York, 1994), Chap. 1.
16. M. A. Arbore, "Application of fundamental-mode cutoff for novel amplifiers and lasers," in *Proc. of OFC 2005, OFB4* (2005).
17. D. S. Gasper, P. F. Wysocki, W. A. Reed, and A. M. Venqsarkar, "Evaluation of chromatic dispersion in erbium-doped fibers," in *Proc. of LEOS 1993, FPW4.2* (1993).
18. N. K. Chen, S. Chi, and S. M. Tseng, "Wideband tunable fiber short-pass filter based on side-polished fiber with dispersive polymer overlay," *Opt. Lett.* **29**, 2219-2221 (2004).
19. H. Ahmad, N. K. Saat, and S. W. Harun, "S-band erbium-doped fiber ring laser using a fiber Bragg grating," *Laser Phys. Lett.* **2**, 369-371 (2005).
20. A. Bellemare, M. Karasek, C. Riviere, F. Babin, G. He, V. Roy, and G. W. Schinn, "A broadly tunable erbium-doped fiber ring laser: experimentation and modeling," *IEEE J. Sel. Top. Quan. Electron.* **7**, 22-29 (2001).
21. J. Yang, S. Dai, N. Dai, L. Wen, L. Hu, and Z. Jiang, "Investigation on nonradiative decay of ⁴I_{13/2} → ⁴I_{15/2} transition of Er³⁺-doped oxide glasses," *J. Lumin.* **106**, 9-14 (2004).
22. S. Sudo, *Optical Fiber Amplifiers: Materials, Devices, and Applications* (Artech House, Boston, 1997), Chap.1.
23. N. K. Chen, S. Chi, and S. M. Tseng, "An efficient local fundamental-mode cutoff for thermo-optic tunable Er³⁺-doped fiber ring laser," *Opt. Express* **13**, 7250-7255 (2005).
24. N. K. Chen and S. Chi, "Novel local liquid-core single mode fiber for dispersion engineering using submicron tapered fiber," in *Proc. of OFC 2007, JThA5* (2007).
25. W. L. Barnes, R. I. Laming, E. J. Tarbox, and P. R. Morkel, "Absorption and emission cross section of Er³⁺ doped silica fibers," *IEEE J. Quan. Electron.* **27**, 1004-1010 (1991).
26. X. S. Jiang, Q. Yang, G. Vienne, Y. H. Li, L. M. Tong, J. J. Zhang, and L. L. Hu, "Demonstration of microfiber knot laser," *Appl. Phys. Lett.* **89**, Art. no. 143513 (2006).

1. Introduction

Wideband tunable fiber laser is not only important for high-bandwidth fiber-optic communication, optical spectroscopy, fiber sensing, but also crucial for biophotonic applications such as optical coherence tomography (OCT) and medical laser surgery. For OCT, a high-tuning-speed fiber laser over a wide spectral range with deep tissue penetration depth at near-infrared wavelengths is necessary. For medical laser surgery, the 1450 nm (diode laser) and 1540 nm (Er:glass laser) wavelengths, for example, are excellent facial resurfacing laser wavelengths to wound the dermis without damaging epidermis so that the fibroblasts are stimulated to produce collagen to improve skin texture within a limiting patient's downtime [1,2]. Moreover, the 755 nm wavelength (Q-switched Alexandrite laser), which could be obtained by frequency doubling from 1510 nm in erbium-doped fiber (EDF), can be efficiently absorbed by chromophore in dermis to remove dermal pigmentation [3,4]. Accordingly, it is advantageous to explore a widely tuning fiber laser over 1450-1540 nm with a high tuning speed based on the high quantum efficiency EDF for cosmetic laser surgery. In order to cover the above wavelength range, it is crucial to extract optical gain in EDF for the wavelengths shorter than the 1480 nm. Usually, the optical gain ranging from 1450 nm to

1480 nm for fiber lasers can be obtained by photon absorption method through the laser transition between ${}^3H_4 \rightarrow {}^3F_4$ multiplet in thulium-doped fiber [5-7], the ${}^4I_{13/2} \rightarrow {}^4I_{15/2}$ multiplet in erbium-doped tellurite fiber [8,9] or by photon inelastic scattering method through the transition between the virtual excited states to ground state in silica Raman fiber [10]. Conventionally, the ${}^4I_{13/2} \rightarrow {}^4I_{15/2}$ multiplet of silica-based EDF at room temperature can only emit fluorescence at the wavelengths longer than 1490 nm [11]. More recently, the silica-based EDF has been utilized to realize optical amplification over S-band (1480-1520 nm) and/or C+L band (1530-1620 nm) [12-14] as a consequence of the influence of Stark splitting on ${}^4I_{13/2}$ and ${}^4I_{15/2}$ multiplets and the introduction of fundamental-mode cutoff in EDF [12,13]. The Stark splitting makes laser transitions of trivalent erbium ions in silica host glass between ${}^4I_{13/2} \rightarrow {}^4I_{15/2}$ multiplets at room temperature can provide optical gain from 1450-1650 nm when the erbium ions are thoroughly inverted [15-17]. A fundamental-mode cutoff mechanism based on waveguide or material dispersion [13, 16, 18] must be employed along EDF to filter out the C+L band amplified spontaneous emission (ASE) so that the optical gain for S-band can be acquired. However, the shortest lasing wavelength of the silica-based EDF fiber laser had been achieved up to date is 1480 nm [19,20]. The major difficulties of obtaining shorter lasing wavelength come from the following two constraints.

First, for erbium ions, the absorption cross section is larger than the emission cross section in S-band and thus the net cross section can only become positive for obtaining net optical gain when at least 80% of the erbium ions are population-inverted under strong optical pumping [15].

Secondly, the population inversion over the excited state multiplet obeys the Boltzmann distribution $e^{-\Delta E/K_B T}$ when atoms are in thermodynamic equilibrium. The ΔE , K_B , and T means the energy separation between Stark sublevels of excited state, Boltzmann constant, and absolute temperature, respectively. The transition rate of the stimulated emission follows the equation $\frac{dN_{2-i}}{dt} = -\frac{\sigma_{2-i} I_{2-i}}{h\nu} N_{2-i}$ and is proportional to N_{2-i} , σ_{2-i} as well as I_{2-i} , where the N_{2-i} , σ_{2-i} ,

and I_{2-i} respectively stands for the number of electrons occupying the i -th sublevel of the excited state, emission cross section of the i -th sublevel of the excited state, and intensity of the transition wavelength from the i -th sublevel of the excited state to ground state. Intuitively, increasing N_{2-i} , I_{2-i} and σ_{2-i} can increase the transition rate for the desired lasing wavelength. Nevertheless, σ_{2-i} is intrinsically determined by the selected host material and the silica glass is known to have a high phonon energy ($\sim 1100 \text{ cm}^{-1}$) which can result in large nonradiative decay rate and low quantum efficiency [21] and thus the resulting σ_{2-i} of silica-based EDF is accordingly very limited. The very limited σ_{2-i} of silica-based EDF for higher energy transition close to the short-wavelength edge of gain bandwidth decreases too rapidly to provide optical gain for the wavelengths shorter than 1480 nm. In silica-based EDF, the σ_{2-i} gradually reduces with decreasing wavelength starting from 1530 nm [11] and the transition rates of C-band wavelengths are larger than that of the S-band wavelengths. Therefore even though it is possible to acquire positive net cross section for the wavelengths shorter than 1480 nm, the net optical gain is still difficult to be obtained. Consequently, a high cutoff efficiency short-pass filters for suppressing the ASE at the wavelengths longer than the lasing wavelength is necessary to squeeze gain out for the wavelength shorter than 1480 nm. In contrast to silica, a low phonon energy glass such as tellurite ($\sim 750 \text{ cm}^{-1}$) or fluoride ($\sim 500 \text{ cm}^{-1}$) glass is a good potential for S-band amplifiers ascribing to its higher erbium solubility and wider σ_{2-i} bandwidth [21]. However, the low phonon energy glass has low compatibility with the popular silica fibers and has higher optical loss because of the ease of crystallization during fiber drawing processes [22]. Regarding to N_{2-i} and I_{2-i} , N_{2-i} is predominately the natural constraint for improving the transition rate for wavelengths shorter than 1480 nm. For the populated electrons staying at the excited state, the Boltzmann distribution plays a role of weighting function and most of the excited electrons occupy the lowest energy sublevels of the excited state. Accordingly, the stimulated emission produced by lower energy photons with longer wavelengths is inherently with a higher transition probability than the higher

energy emission. However, the transition rate for the electrons at the higher energy sublevels of the excited state could be enhanced by suppressing the growth of ASE at the longer wavelengths by using fundamental-mode cutoff filters. By doing so, the stimulated photons with higher energy transition can make the electrons at higher energy sublevels quickly drop to ground state and subsequently be pumped to fill into the higher energy sublevels of the excited state once more to satisfy the Boltzmann's law. In accordance, the I_{2-i} of the higher energy stimulated photons can thus rapidly increase to enhance the transition rate again and to squeeze out more optical gains for the shorter wavelengths.

In this paper, we employ wideband tunable high cutoff efficiency fused-tapered short-pass filters discretely located in a standard silica-based C-band EDF as shown in Fig. 1. The fiber laser can be tuned over 1451.9-1548.1 nm with the temperature tuning efficiency as high as 57.3 nm/°C. To our best knowledge, this is the first time that a silica-based EDF fiber laser can lase so close to the short-wavelength limit of 1450 nm and can be tuned with such a high efficiency over a wide spectral range.

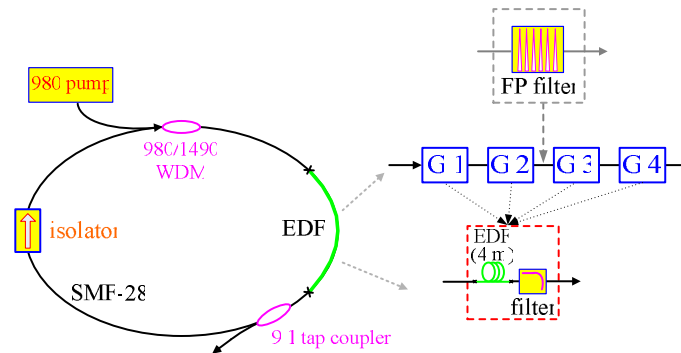


Fig. 1. Experimental set-up of the tunable EDF ring laser towards the short-wavelength limit at 1450 nm. Each 4-m-long EDF and short-pass filter forms a gain stage and there are four gain stages totally in the ring cavity. The FP filter is used for narrowing the laser linewidth down below 0.2 nm.

2. Fabrication and experiments

In order to explore what is the shortest lasing wavelength that can be achieved in a silica-based EDF, fundamental-mode cutoff filters with sharp filter skirt and deep stopband are necessary. Both of the material dispersion and waveguide dispersion of the tapered fiber are crucial for the cutoff efficiency (slope of the roll-off curve). In terms of the material and waveguide dispersion, a larger cross angle between the refractive index dispersion curves of the silica fiber and the optical liquid [23] and a longer uniform waist with a suitable tapered diameter [24] can result in higher cutoff efficiency for the short-pass filters employed in this experiment. The experimental set-up of the tunable EDF ring laser is shown in Fig. 1, where the tunable fused-tapered short-pass filters are fabricated by tapering the single-mode fiber (Corning: SMF-28) down to the diameter and length around 30 μm and 22 mm respectively by using the moving hydrogen flame. Two sets of four tapered fibers are prepared and their spectral responses are measured by using superluminescent diodes covering 1250-1650 nm wavelengths and an optical spectrum analyzer under optical resolution (RES) of 1 nm. Four tapered fibers are made for each run and they are individually glued into the grooves of glass substrate and covered by the Cargille index liquid ($n_D = 1.456$) [12] to achieve the rejection ratio of 50 dB for stopband and the cutoff efficiency of -1.02 dB/nm as shown in Figs. 2(a) and 2(b). Two thermoelectric coolers (TECs) with temperature resolution of 0.1°C are stacked up and placed beneath the glass substrate to efficiently vary the cutoff wavelength ascribing to the large thermo-optic coefficient $dn_D/dT = -3.74 \times 10^{-4}/^\circ\text{C}$ of the optical liquid. From Figs. 2(a) and 2(b), the wavelength mismatch among the four short-pass filters is smaller than 5.9

nm even when the cutoff wavelength is tuned beyond one hundred nanometers. The best tuning efficiency η of the cutoff wavelength is measured to be 58.8 nm/°C and the same cutoff efficiency can be maintained at different temperatures. The hydroxyl ions coming from the hydrogen flame diffusing into the tapered fiber cause the excess loss of a few dB around 1390 nm and can be further avoided by using OH⁻ free heating source such as CO₂ laser. The environment stability for the spectral responses is good by using the dual TECs. In contrast to the fundamental-mode cutoff resulting from waveguide dispersion by employing the depressed inner cladding structure in EDF [13,14,16,19], the present fundamental-mode cutoff filters based on the tapered fibers surrounded by low phonon energy optical liquid [12] is superior on the respects of higher cutoff efficiency over a much wider tuning range (at least wider than 1250-1650 nm) with no moving part and high tuning efficiency. The four filters are discretely spliced into a 16-m-long standard silica-based C-band EDF (Prime Optical Fiber Corporation: EDFH0790) to substantially suppress the ASE at the wavelengths longer than the lasing wavelength, which can be tuned by varying the applied temperature on the short-pass filters. The EDFH0790 uses an aluminosilicate host glass in which the aluminum ions serve as modifier ions to open the tightly linked SiO₂ network for more erbium ions solubility and significantly reduce the large gap between the emission cross sections of S- and C-band wavelengths [25], so that the difficulties in increasing transition rate for S-band wavelengths as previously mentioned can be highly alleviated and the quantum efficiency for the S-band wavelengths can be improved. Since the fundamental-mode cutoff filters are discretely introduced along the EDF to filter out the unwanted C-band ASE for enhancing the transition probability of S-band wavelengths, each filter is used for every 4-m-long EDF to form a gain stage and thus the ring laser comprises four gain stages (G1 ~ G4) as shown in Fig. 1. The reason of using 4-m-long EDF for each gain stage is judged by experimentally launching a 1490 nm DFB (distributed feedback) laser signal with 1 μW power into several highly inverted EDFs with different lengths and the EDF length that can achieve the highest gain is selected. High power 980 nm pump lights are launched into the ring cavity through a 980/1490 WDM coupler to achieve high population inversion along the entire 16-m-long EDF and a 9:1 tap coupler is used as the laser output coupler. In the first experiment, the first set of tapered fibers is used in ring laser to explore the shortest wavelength that can be reached over $^4I_{13/2} \rightarrow ^4I_{15/2}$ transition, whereas in the second experiment an additional Fabry-Perot (FP) filter is inserted between the two adjacent filters of the second set of the tapered fibers to narrow down the laser linewidth and to improve the signal-ASE-ratio. The spectral responses of the FP filter is shown in Fig. 2(c), where the 3 dB bandwidth (3 dB $\Delta\lambda$) for passband and the free spectral range (FSR) of the FP filter is 0.2 nm and 50 nm respectively. The peak wavelength of the passband can be moved for 23.8 nm around the 1450 nm wavelength and for 16.1 nm around the 1550 nm wavelength, all toward the longer wavelength when a voltage of 5 V is applied. The insertion loss of the FP filter is about 1.35 dB over the S- and C-band range and the splicing loss between EDFH0790 and SMF-28 is 0.35 dB due to the mismatch of numerical aperture [12]. A broadband in-line isolator with the isolation of 35 dB from 1450 nm to 1650 nm is used to achieve unidirectional lasing.

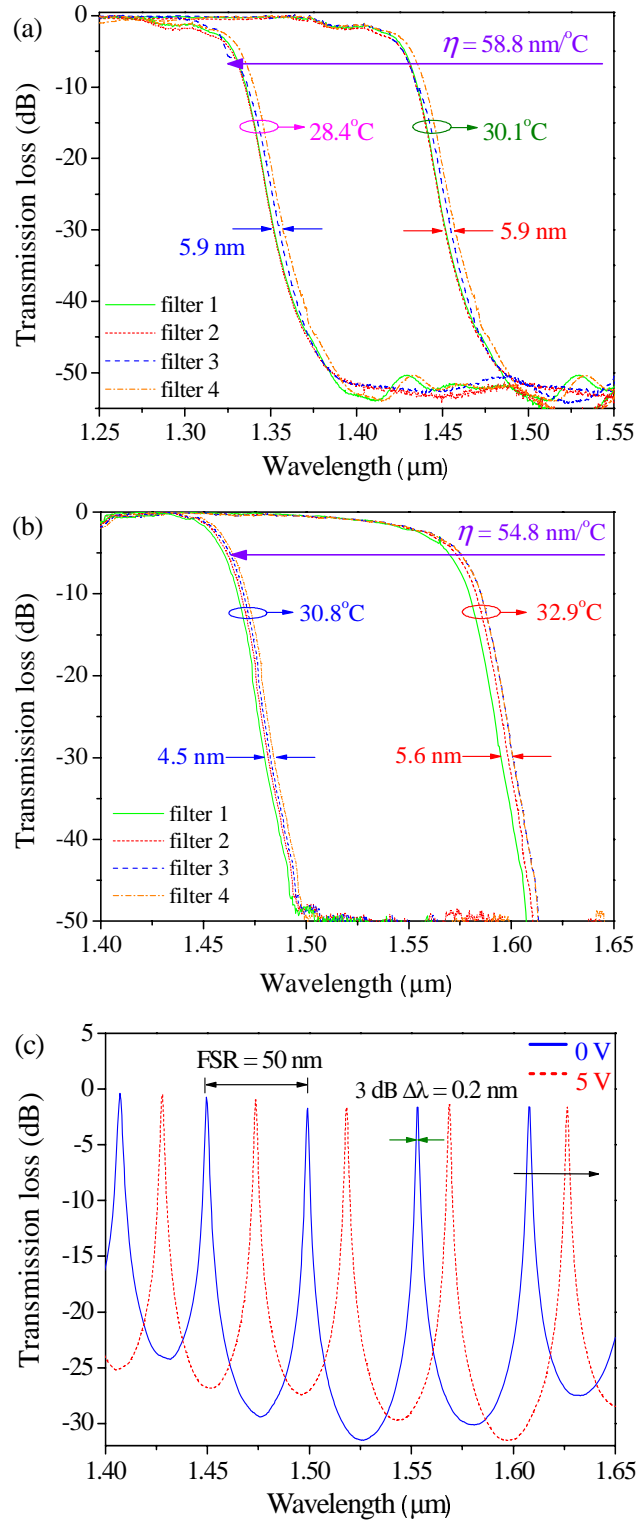


Fig. 2. Spectral responses of the grouped four tapered fiber short-pass filters covered by Cargille liquid ($n_D = 1.456$) at different temperatures (RES: 1 nm) for (a) the first set and (b) the second set. (c) Transmission spectra of the FP filter at different applying electric voltages (RES: 1 nm).

3. Results and discussions

For the EDF ring lasers, the initial generated ASE at free running are of course covering S-, C-, and L-bands and the lasing wavelength is self-determined by the gain/loss spectrum and resonant conditions of the ring cavity. Moreover, the tunable short-pass filters along the 16-m-long EDF can modify the gain shape as well by filtering out the wavelengths longer than the lasing wavelength. Since the cutoff wavelength can be tuning toward the shorter wavelength when the applying temperature is cooled down, the lasing wavelength of the EDF ring laser can thus be forced to move toward shorter wavelengths. In the first experiment, a 980 nm pump power of 208 mW is launching into the EDF and the corresponding laser spectra under the RES of 0.1 nm at different temperatures are shown in Fig. 3(a). In the beginning, the temperature for short-pass filters is tuned to be 30.9°C. The ASE is free running in the ring cavity and the lasing wavelength is automatically selected at 1545.2 nm. While the applied temperature is gradually decreased, the lasing wavelength can move to as short as 1451.9 nm, which is believed to be the shortest lasing wavelength over ${}^4I_{13/2} \rightarrow {}^4I_{15/2}$ transition in silica-based EDFs that has been reported to date. The average η for the tunable laser is measured to be as high as 57.3 nm/°C from 1545.2 to 1451.9 nm, which is quite consistent to that of the short-pass filters. The laser peak power slowly drops with the decreasing lasing wavelength since the positive net cross section of the erbium ions becomes more and more difficult to obtain when the wavelength gradually goes down. Therefore, it is very important to make the entire 16-m-long EDF fully inverted to obtain the lasing wavelength as short as possible. At the wavelengths shorter than 1451.9 nm, the optical gain is insufficient to support lasing there. The average full width at half maximum (FWHM) of the laser is 0.53 nm and the signal-ASE-ratio is about 40 dB. At 30.9°C, two small fiber segments in the 16-m-long EDF are bent with a diameter of 0.85 cm at the location of 4.5 cm away from one splicing point between EDF and SMF-28 to change the resonance conditions of ring cavity. The lasing wavelength moves from 1545.2 nm to 1548.1 nm since the length of resonant cavity is slightly elongated.

Based on the same scheme, in the second experiment an additional FP filter is inserted in between two adjacent filters of the second set of tapered filters while the pump power is raised to 227 mW. The corresponding laser spectra under the RES of 0.1 nm are shown in Fig. 3(b). Without using the FP filter, the initial laser occurs at 1565 nm at 36.2°C and moves to 1462.2 nm at 29.4°C. The temperature tuning efficiency is seen to be 15.12 nm/°C only. However, the short-pass filter at 36.2°C plays as an all-pass filter and thus the tuning efficiency can not reflect the real tuning ability for the ring laser. At 36.2°C, the lasing wavelength moves to 1556.3 nm when a FP filter is employed in the ring cavity. The laser subsequently moves to 1573.2 nm when the FP filter is operated under a voltage of 5V. The laser can be tuned by controlling either the FP filter or the short-pass filters and can respectively jump to the wavelength of 1520.1 nm and 1525.1 nm when the voltage of FP filter is zero and 5V under the temperature of 30.5°C. In order to search the shortest wavelength that can be obtained for the ring laser using the second set of tapered filters, the applying temperature for short-pass filters and the voltage for FP filter are carefully tuned to achieve a shortest wavelength at 1456.3 nm under the temperature and voltage of 29.2°C and 1.1V, respectively. At 1456.3 nm, the laser output power, the FWHM, the 20 dB linewidth, and the signal-ASE-ratio are measured to be 61.52 μ W (-12.11 dBm), 0.15 nm, 0.47 nm, and higher than 45 dB, respectively. In contrast to Fig. 3(a), the spectral narrowing of laser linewidth is mainly contributed by the FP filter and the 20 dB linewidth at 1456.3 nm is even smaller than the FWHM of the laser without using FP filter. At 1456.3 nm, the laser output power drops from 61.52 μ W (-12.11 dBm) to 50.9 μ W (-12.93 dBm) in accordance with the pump power decreasing from 227 mW to 212 mW. The average slope efficiency for EDF lasing at 1456.3 nm is 0.0255%. In the second experiment, the longest and the shortest lasing wavelengths are 1573.2 nm and 1456.3 nm, respectively. The tuning range is 116.9 nm within the temperature variations of 7°C for short-pass filters and the voltage variations of 5V for the FP filter. Based

on the temperature stability of 0.1°C , the fluctuation of laser output power is less than 1.21 dB and the lasing wavelength can be fixed in a few tens of minutes of testing when an FP filter is used. Without the FP filter, the output power can even fluctuate for more than 2.5 dB and the lasing wavelength is difficult to be fixed for more than ten minutes. Clearly, by combining the discrete short-pass filters and FP filter in EDF ring cavity, an EDF laser with high tuning efficiency, wide tuning range, narrow laser linewidth and high signal-ASE-ratio is highly promising. In addition, it could be possible to achieve a shorter lasing wavelength by employing a high Q cavity such as using microring or microknot filters [26]. A high Q cavity can also help achieving narrow linewidth to distinguish the laser light from other neighboring wavelengths. Hence, the laser light can be moved to even shorter wavelengths when a high Q cavity is further employed to investigate the real short-wavelength lasing limit over ${}^4I_{13/2} \rightarrow {}^4I_{15/2}$ transition in silica-based EDF.

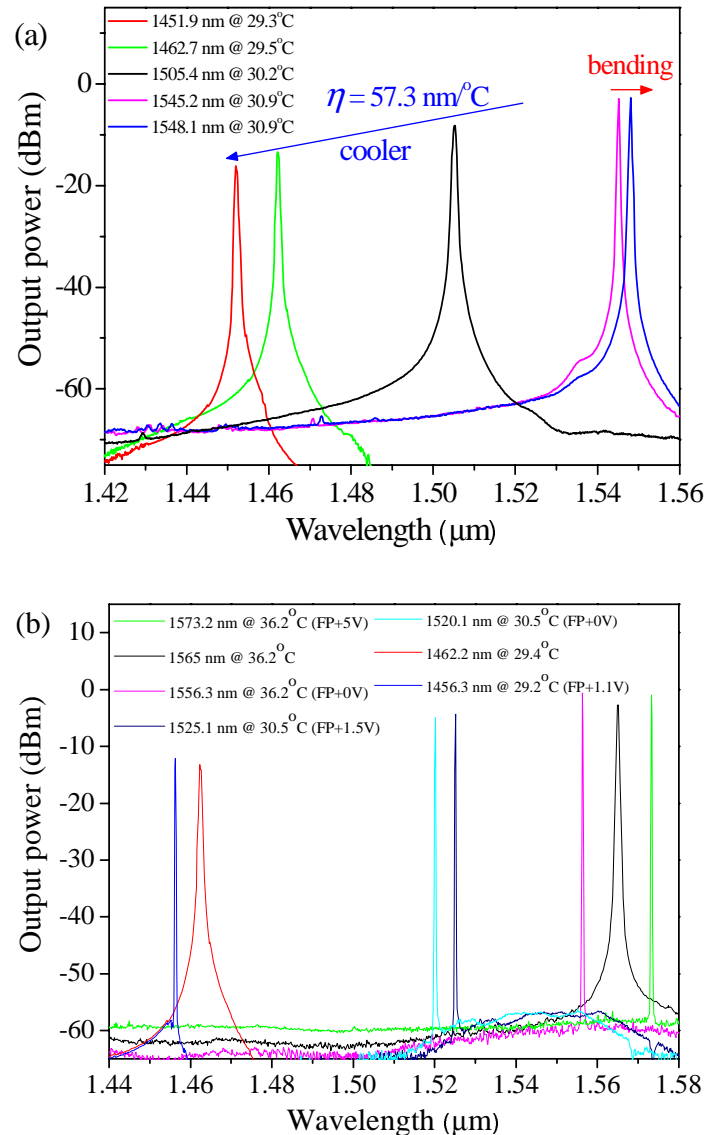


Fig. 3. Evolution of the output laser spectra by (a) cooling down the optical liquid and bending the splicing point using the first set of tapered fibers (RES: 0.1 nm) and by (b) cooling down the optical liquid and tuning the FP filter using the second set of tapered fibers (RES: 0.1 nm).

4. Conclusion

In conclusion, we have demonstrated that the ${}^4I_{13/2} \rightarrow {}^4I_{15/2}$ transition in silica-based EDF can indeed provide optical gain at the wavelength very close to 1450 nm when the EDF is thoroughly inverted and a fundamental-mode cutoff mechanism is introduced. A widely tunable EDF ring laser with the temperature tuning efficiency as high as 57.3 nm/°C over 1451.9-1548.1 nm wavelength by using a 16-m-long standard C-band silica-based EDF under the 980 nm pump power of a little higher than 200 mW is achieved. The signal-ASE-ratio is higher than 45 dB and the FWHM of laser is about 0.53 nm and can be narrowed down below 0.2 nm by incorporating a Fabry-Perot filter into the ring cavity. The laser linewidth can be further narrowed and the lasing wavelength is believed to be capable of tuning toward the wavelengths even shorter than 1450 nm by using an ultra-high Q microring resonator and distributed fundamental-mode cutoff in EDF in the future. The slope efficiency of lasing near 1450 nm wavelength could also be improved by introducing distributed fundamental-mode cutoff which can remove the unwanted C+L band ASE at the same time when they are generated and thus significantly suppresses the energy transfer from the pump power into unwanted ASE. The laser output power can be further scaled up based on a master oscillator power amplifier scheme. This widely tunable erbium-doped fiber laser with high tuning efficiency is simple, cost-effective, and should be beneficial to the broadband fiber-optic communication, spectroscopy, and fiber-optic laser surgery applications.

Acknowledgments

This work was funded by grants from the Republic of China National Science Council (NSC 95-2752-E-009-009-PAE & NSC 95-2221-E-155-072) and National Chiao Tung University (MOE ATU Program).